An operational optimization method for a complex polygeneration plant based on real-time measurements

L. Urbanucci[1*], D. Testi[1] and J. C. Bruno[2]

[1]DESTEC (Department of Energy, Systems, Territory and Constructions Engineering), University of Pisa, Largo L. Lazzarino, 56122 Pisa, Italy

[2]Department of Mechanical Engineering, University Rovira i Virgili, Avda. Països Catalans 26, Tarragona 43007, Spain

[*]Corresponding author: luca.urbanucci@ing.unipi.it

Abstract

The combined production of electricity, heat and cold by a polygeneration system connected to a district heating and cooling network can provide high energy utilization efficiency. The inherent complexity of simultaneous production of different services and the high variability in the energy demand make combined cooling and heating systems performance highly dependent on the operational strategy. In this paper, an operational optimization method based on the moving average of real-time measurements of energy demands and ambient conditions is proposed. Real energy demand data from a district heating and cooling network close to Barcelona, Spain, are used to test the method. A complex polygeneration system is considered, consisting of an internal combustion engine, a double-effect absorption chiller, an electric chiller, a boiler and a cooling tower. A detailed modelling of the system is provided, considering partial load behavior of the components and ambient conditions effects. Results of the real-time optimal management are discussed and compared to traditional operational strategies and to the ideal optimal management achievable with

perfectly accurate forecast of energy demands. Moreover, the optimal width of the window adopted for the moving average of real-time data is identified.

Keywords

Combined Cooling Heat and Power

District Heating and Cooling

Real-time optimization

Operational optimization

Partial load

Real-time data

1. Introduction

Combined Cooling, Heating and Power (CCHP) systems are proven to be a reliable, competitive and very efficient alternative to separate production. CCHP is a common configuration for distributed energy systems where the end users are close to the energy generation point. These systems can be connected to a District Heating and Cooling (DHC) network [1], which is an energy efficient and environmentally benign solution compared to decentralized heat generation [2]. Nevertheless, the energy, environmental and economic performances of CCHP systems are strongly influenced by system synthesis [3], equipment selection and capacity [4] and operational strategy [5].

Different optimization techniques have been adopted over the years in order to identify the optimal design of polygeneration systems [6]. Arcuri et al. [7] presented a Mixed Integer Linear Programming (MILP) model for the determination of the design and the running conditions of a trigeneration plant for a hospital complex. Guo et al. [8] carried out a two-stage optimal planning and design method for a CCHP microgrid system, using both genetic algorithm and MILP

algorithm techniques. Elsido et al. [9] and Arcuri et al. [10] proposed Mixed-Integer Non-Linear Programming models for determining the most profitable synthesis, design and annual scheduling of cogeneration systems.

Other works have focused on the optimal exploitation of the CCHP potential in existing plants. Franco and Versace [11] defined an optimal operational strategy for a cogeneration plant connected to a District Heating System. Li et al. [12] analyzed the effect of optimized operational strategy on a CCHP system for office and residential buildings. Ortiga et al. [13] presented a scenario analysis for economic, energetic and environmental performance assessment of a polygeneration system connected to a DHC network. Bischi et al. [14], Perez-Mora et al. [1] and Ünal et al. [15] investigated the optimal operating schedule of CCHP systems, with a given design.

Such works are usually based on an accurate load profile, while in practical applications an estimate of future load profile must be made [16]. Therefore, in order to implement optimal operational strategies in actual polygeneration systems, several methods have been proposed based on both demand forecast and real-time information. Fang and Lahdelma [17] developed a model based on weather and power price forecast and a sliding time window optimization. Luo et al. [18] provided a two-stage control for CCHP microgrid, including a Model Predictive Control (MPC) based on forecast information and a real-time adjusting stage to tackle power fluctuations. Cho et al. [19] and Yun et al. [20] tested real-time cost optimization algorithms on case studies.

Advanced control algorithms for real-time operations of CCHP systems have become a subject of great interest [21]. Uncertainties in energy demand forecast, non-linear part-load performances, multiple time-varying loads and various economical feature make the optimal management of polygeneration plants very challenging. In particular, savings resulting from real-time control are very dependent on the accuracy of the forecasts [17], while, in addition, accurate local weather predictions may be difficult to obtain [20]. Moreover, building simulation models are

needed to estimate the thermal loads [19] and the calibration of the building model to the actual building may be an additional obstacle for real implementation of optimal control algorithms [20].

In this paper, an original operational optimization method based on real-time measurements of energy demands and ambient conditions is defined. The main novelty of this study is that the proposed method needs neither weather forecast nor a model for the estimation of future energy load demands, but only a monitoring system of the polygeneration plant. A moving average of real-time measurements of energy loads and current dry-bulb temperature and relative humidity are used to estimate energy load demands and energy system performance. On this basis, an optimal operational strategy is defined and, subsequently, a post-strategy design compensates for the gap between the estimated and the actual data.

The method is demonstrated by using real energy demand data from a trigeneration plant connected to a DHC network close to Barcelona (Spain). The energy system under investigation comprises an internal combustion engine, a double-effect absorption chiller, an electric chiller, a boiler and a cooling tower. An extensive modelling of the equipment is provided, considering partial load behaviour and ambient conditions effects, to perform realistic and detailed simulations of the energy system.

The energy dispatch algorithm is designed to minimize the cost of energy (i.e. cost for purchasing electricity from the grid, income for selling electricity to the grid, cost of natural gas). To validate and evaluate the efficiency of the method, it is compared to conventional operational strategies and to the ideal optimal management achievable with perfectly accurate forecast of energy demands. Moreover, the effect of the width of the window adopted for the moving average on the performance of the method is analysed and the optimal width is identified.

The rest of this paper is structured as follows. In Section 2 the methodological framework is described in detail. Section 3 presents the case study and the modelling of the energy system. An in-depth analysis of the results follows in Section 4, while the last section contains concluding remarks.

2. Methodology

A Real-Time Operational Optimization (RTOO) procedure based on measurements of energy demands and ambient conditions is proposed. The aim of this method is to determine an operational strategy that can be implemented in real-time to define the optimal energy input and flow inside the system. In this regard, a specific methodological framework has been developed, which is presented in this section.

The energy system under investigation is a typical CCHP system [4], consisting of an internal combustion engine, an absorption chiller, an electric chiller, a boiler and a cooling tower. The power plant feeds electricity to the grid, and heating and cooling to a DHC network. The energy system configuration is schematically shown in Fig. 4. Its operations are illustrated in detail in Section 3.2.

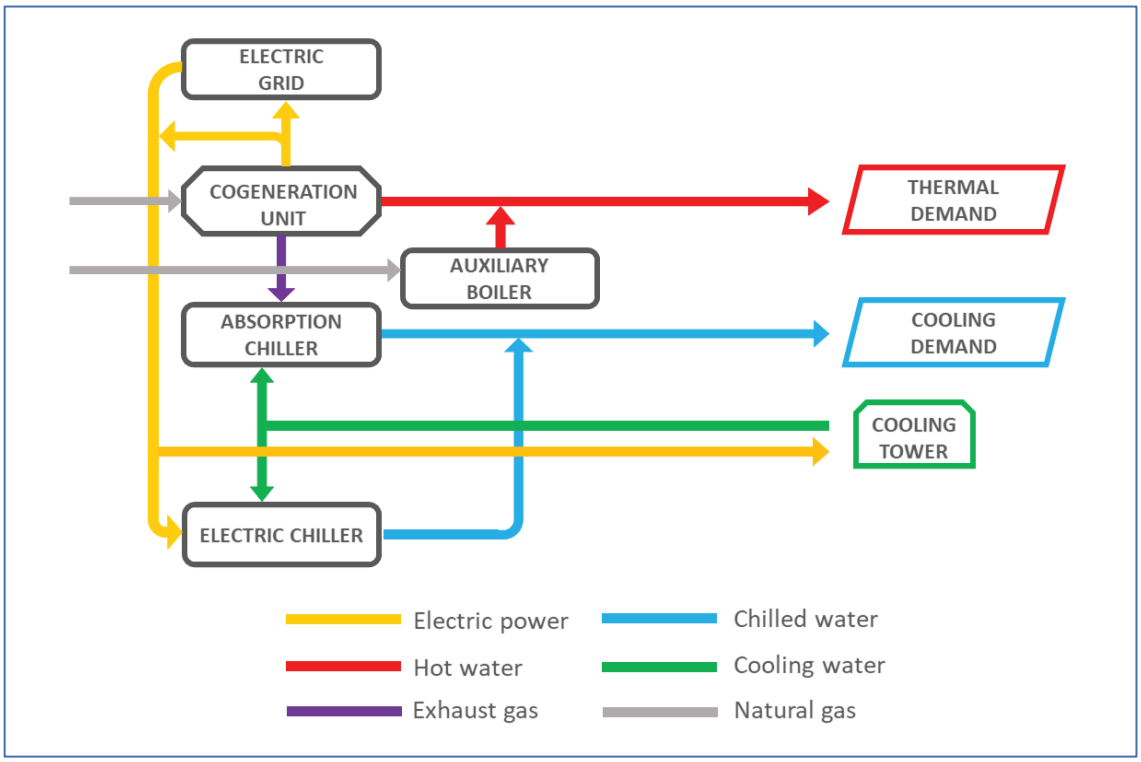

Fig. 4. Schematic representation of the Combined Cooling Heat and Power system

2.1 The objective function

The optimization problem consists in the determination of the scheduling that meets the energy demand with the lowest possible cost. For the energy system under consideration, the economic features to be accounted for are: the purchased natural gas price, both for the boiler and the internal combustion engine, the price for purchasing electricity by the grid, both for the electric chiller and the cooling tower, and the income for selling to the grid the remaining electricity produced by the ICE.

The total energy cost for the considered period (n timesteps) is therefore defined as follows

$$EC = \sum_{i=1}^{n} c_F^i F_{boi}^i + \sum_{i=1}^{n} c_F^i F_{ICE}^i + \sum_{i=1}^{n} c_{PEG}^i E_P^i - \sum_{i=1}^{n} c_{SEG}^i E_S^i \tag{8}$$

where F_{boi} and F_{ICE} are the fuel consumed by the boiler and the ICE, respectively, and E_P and E_S are the purchased and sold electric energy, respectively. Finally, the optimization problem consists in the minimization of this quantity:

$$min\{EC\}. \tag{9}$$

2.2 Decision variables, demand constraints, capacity constraints and balance equations

As a consequence, the following eight decision variables are defined for the *i*-th timestep: $E_{ICE}^i, Q_{HT,ICE}^i, Q_{LT,ICE}^i, Q_{LT,boi}^i, E_S^i, E_P^i, C_{EC}^i, C_{AC}^i$.

Demand constraints for both hot water and chilled water are defined as follows:

$$Q_{LT,ICE}^i + Q_{LT,boi}^i - Q_{LT,D}^i \geq 0 \tag{10}$$

$$C_{EC}^i + C_{AC}^i - C_D^i = 0 \tag{11}$$

where $i = 1, 2, \dots, n$.

The following balance equations and inequalities are considered.

$$F_{ICE}^i - {E_{ICE}^i}/{\eta_{E,ICE}^i} = 0 \tag{12}$$

$$Q_{HT,ICE}^{i} - E_{ICE}^{i} \frac{\eta_{Q,HT,ICE}^{i}}{\eta_{E,ICE}^{i}} = 0 \tag{13}$$

$$Q_{LT,ICE}^{i} - E_{ICE}^{i} \frac{\eta_{Q,LT,ICE}^{i}}{\eta_{E,ICE}^{i}} = 0 \tag{14}$$

$$E_{EC}^{i} - \frac{C_{EC}^{i}}{COP_{EC}^{i}} = 0 \tag{15}$$

$$Q_{HT,AC}^{i} - \frac{C_{AC}^{i}}{COP_{AC}^{i}} = 0 \tag{16}$$

$$Q_{HT,AC}^{i} - Q_{HT,ICE}^{i} \leq 0 \tag{17}$$

$$F_{boi}^{i} - \frac{Q_{boi}^{i}}{\eta_{boi}^{i}} = 0 \tag{18}$$

$$W_{CT}^{i} = E_{EC}^{i}\left(COP_{EC}^{i} + 1\right) + Q_{HT,AC}^{i}\left(COP_{AC}^{i} + 1\right) + \max\left\{Q_{LT,ICE}^{i} - Q_{D}^{i}, 0\right\} \tag{19}$$

$$E_{CT}^{i} = f_{CT} W_{CT}^{i} \tag{20}$$

$$E_{P}^{i} = \max\left\{E_{CT}^{i} + E_{EC}^{i} - E_{ICE}^{i}, 0\right\} \tag{21}$$

$$E_S^i = \max\left\{E_{ICE}^i - E_{CT}^i - E_{EC}^i, 0\right\} \tag{22}$$

where $i = 1, 2, \dots, n$. In particular, equations (19,20) define the heat dissipation requirement to the cooling tower and its electric energy consumption, while equations (21,22) state that in the *i*-th timestep electricity is either sold or purchased.

Capacity constraints are defined as follows:

$$E_{ICE}^i - E_{ICE,nom}\delta_{ICE}^i \leq 0 \tag{23}$$

$$E_{ICE}^i - E_{ICE,min}\delta_{ICE}^i \geq 0 \tag{24}$$

$$C_{EC}^i - C_{EC,nom}^i\delta_{ICE}^i \leq 0 \tag{25}$$

$$C_{EC}^i - C_{EC,min}^i\delta_{EC}^i \geq 0 \tag{26}$$

$$C_{AC}^i - C_{AC,nom}^i\delta_{ICE}^i \leq 0 \tag{27}$$

$$C_{AC}^{i} - C_{AC,min}^{i}\delta_{AC}^{i} \geq 0 \tag{28}$$

$$Q_{LT,boi}^{i} - Q_{LT,boi,nom}\delta_{boi}^{i} \leq 0 \tag{29}$$

where $i = 1, 2, \ldots, n$, and δ_{m}^{i} are binary variables equal to 1 when the m-th system component is on and equal to 0 when it is off. Therefore, equations (23,25,27,29) define the maximum output capacity of the relevant machine, and equations (24,26,28) impose that the minimum allowable load factors are respected.

2.3 Optimal energy dispatch strategy

Even though there are eight decision variables, there is only one actual degree of freedom for the minimization of the objective function. The problem is reduced to find the optimal load factor, L_{ICE}, of the internal combustion engine, for each timestep. In fact, once the L_{ICE} is set, the amount of electric energy, high-temperature heat and low-temperature heat produced by the ICE is defined. As a consequence, equation (10) states that the boiler production must meet the remaining hot water demand, if any. Furthermore, once a certain amount of high-temperature heat is produced by the ICE, the absorption chiller should produce the maximum amount of cooling energy, until the chilled water demand is met, if possible. There would be no purpose, indeed, in wasting the available high-temperature heat. In addition, equation (11) entails that the electric chiller must meet the remaining chilled water demand, if any. Therefore, the electric energy exchange with the grid is also defined from equations (21,22) and, as mentioned, the eight decision variables are bound to the load factor of the internal combustion engine. This procedure is summarized in the diagram set forth in Fig. 9.

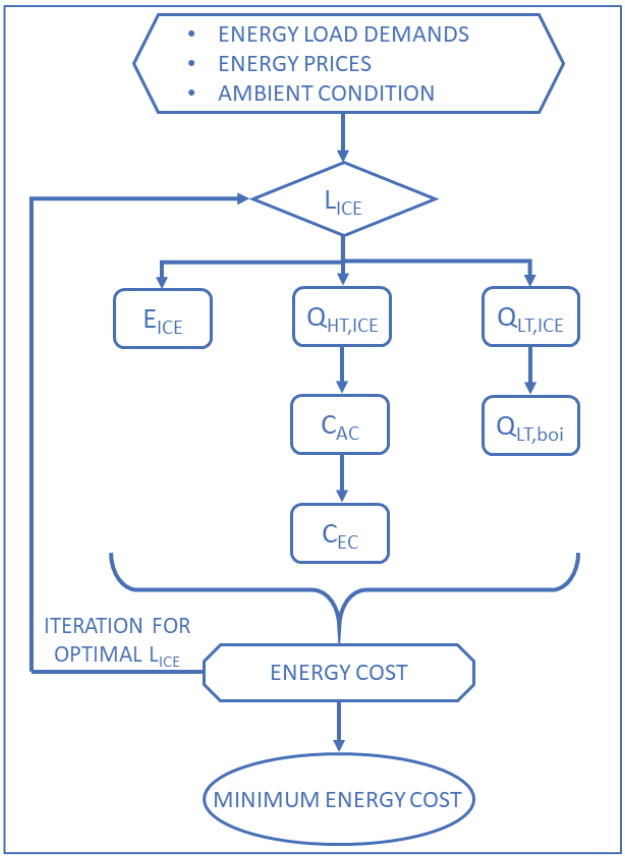

Fig. 9. Optimal energy dispatch procedure

Thus, this optimization algorithm is aimed at identifying, for each simulated timestep, the optimal load factor of the cogeneration unit that minimizes the overall energy cost for the accounted period. For this purpose, several optimization techniques have been used over the years, such as mathematical programming, genetic algorithms and other methods [22]. Usually, these algorithms investigate the entire feasible region, considering a single optimization problem for the whole-time domain, thus requiring high computational cost [23] and long-term forecast. Nevertheless, for the energy system under consideration, the overall optimum coincides with the sum of optimums of every single timestep. As already shown in [23], the so-called "greedy approach" can be used because the physical system has no "memory" of the previous timesteps. Therefore, the overall problem can be split into *n* subproblems, one for each 15-minute timestep, and a low computational-cost algorithm, compatible with the need of a quick response for a real-time

implementation, was specifically written. Consequently, the optimal load factor for each time-step can be independently calculated and then implemented in the system.

Up to now, the energy load demands have been considered as if they were perfectly known, but that is not the case in practical applications. In fact, an estimation of the hot and chilled water demands for the forthcoming timestep is needed. As cited above, several approaches based on weather forecast can be found in literature [17-20], whose shortcomings have already been discussed. Conversely, with the present system configuration, the real-time information made available by the monitoring system of the polygeneration plant can be used.

In particular, previous measurements of energy demands are used to estimate future loads by means of a sliding window of moving average. The width of the window should be optimized, too. For example, in our case (which is presented in Section 3), the energy demand measurements are available on a minute-by-minute basis and the last value measured might be an outlier. In fact, fluctuations on both the actual energy demands and due to sampling errors on the measured values may occur. On the other hand, considering too many past values can be misleading, since they do not represent the current demand. For these reasons an average value of recently measured data is used to estimate the load demands in the following timestep.

Moreover, such a methodology considers current ambient conditions, which can significantly affect chillers performance, and, subsequently, allows to optimally control these devices.

In summary, the energy demands for each timestep are estimated by means of the moving average of recent measures and current ambient conditions, then the optimal load factor for the cogeneration unit is found and the resulting power flows inside the system are determined and implemented in the following timestep.

2.4 Post-strategy design

Nevertheless, there might exist discrepancies between the estimated and the actual loads during each timestep. Thus, purchasing additional primary energy, or selling back or discarding the excess energy are needed [24]. In other words, a post-strategy design is needed.

As shown in [25], several cases, on the basis of the relationship between the forecasted loads and the actual ones, may occur. In particular, if the hot water production by the ICE or the chilled water produced by the absorption chiller exceed the demand, no action needs to be taken and this part of energy will be wasted. Of course, if there is a surplus of electric energy, it will be sold to the grid. If instead the hot water production is not enough to meet the demand, additional fuel must be purchased to run the boiler. Again, if the chilled water production is not sufficient to satisfy the demand, the gap must be filled up by the electric chiller, either utilizing the electric energy produced by the ICE or purchasing additional electric energy from the grid.

3. Case study presentation

To test the above-mentioned methodology and make it easily understandable, a case study is used for testing it. In this section, the energy system under investigation and the load demands of the case study are shown.

3.1 Energy load demand

Real energy demand data from a polygeneration plant connected to a DHC close to Barcelona (Spain) [26] are used to test the method. The supervision of the entire plant is made possible by a dense network of sensors that measure temperature, flow and power values every minute. The monitoring system is described in detail in [27]. The total monitoring system is composed of 150 sensors: 100 temperature sensors, 27 flow sensors, 13 power sensors, and 10 valve sensors. The data acquisition system can record multiple variables in short sampling times

and therefore the volume of available information is very large and allows the definition of each power flow. In particular, temperature and flow data from sensors located in the chilled water and hot water circuits are used to evaluate the energy demands.

The considered energy load data consist of hot water demand (at 90 °C) and chilled water demand (at 5 °C) and are available on a minute-by-minute basis for a whole summer period (166 consecutive days from May 1, 2013 to October 13, 2013). Data are described in summary in Table 1 and in Figs. 1-3.

Table 1

Energy demand summary

	Chilled water demand	Hot water demand
Average [kW]	3009	90
Peak [kW]	6401	688

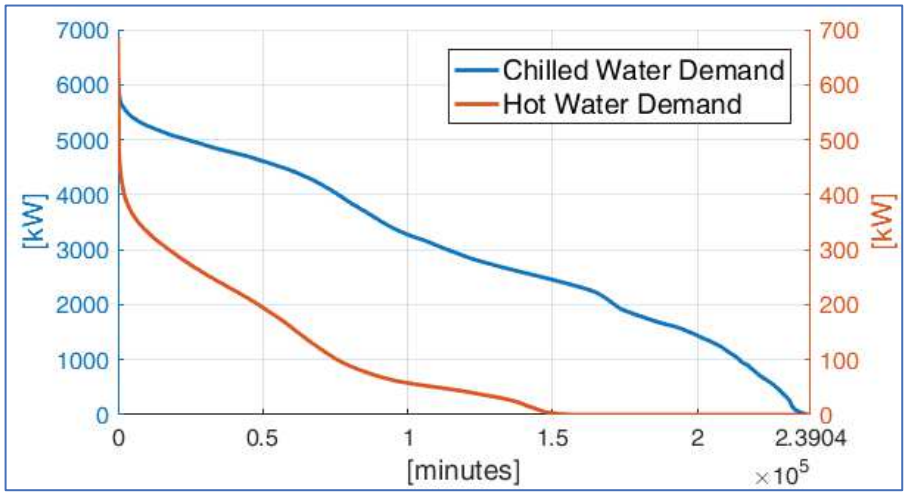

Fig. 1. Chilled and hot water demand: load duration curves

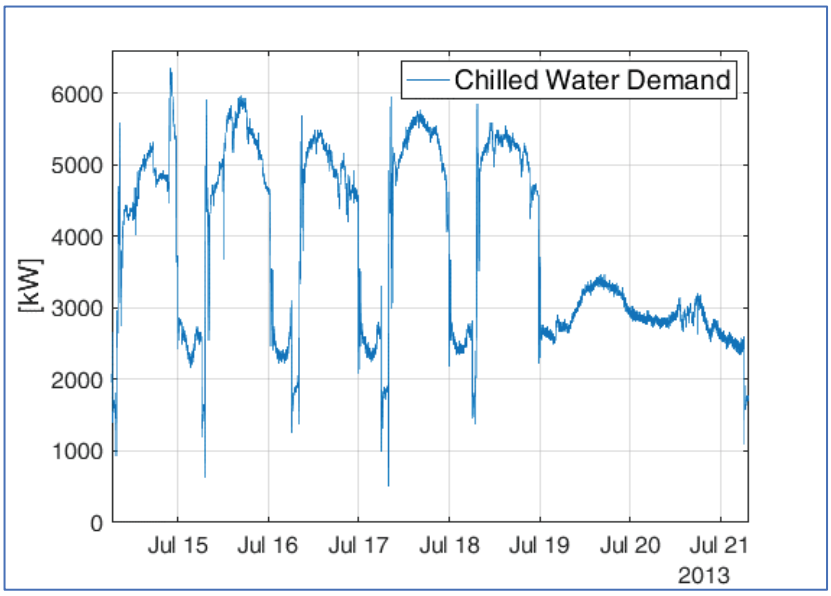

Fig. 2. Chilled water demand: a typical week

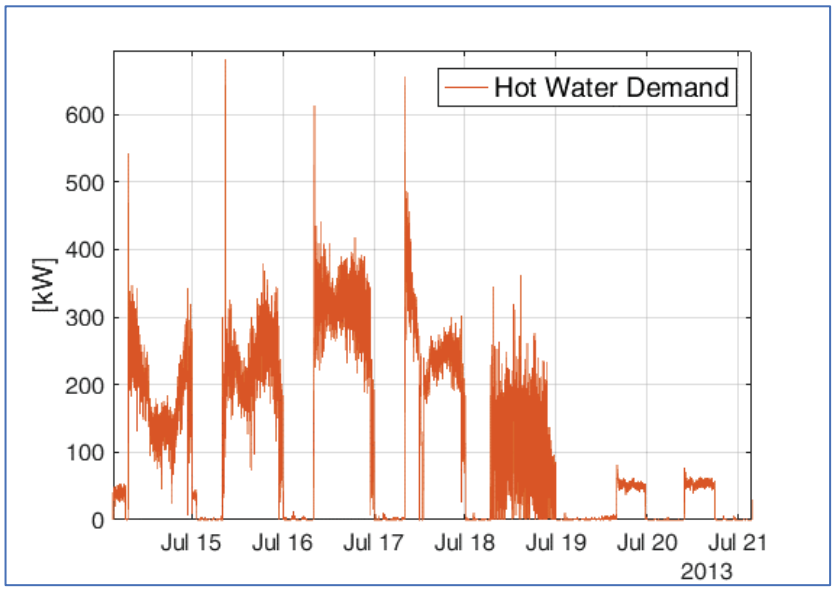

Fig. 3. Hot water demand: a typical week

3.2 The energy system: technical and economic characterization

In this section, models and features adopted for the components of the simulated energy system are described.

3.2.1 Cogeneration unit

The chosen cogeneration unit is a spark-ignition reciprocating internal combustion engine (ICE) fueled by natural gas. The nominal electric power capacity of the ICE is equal to 2800 kW. The electric power generated is used in the first place for the internal consumption of the plant, while the remaining part is sold to the electric grid.

The heat recovery system of the ICE is characterized by a low-temperature level (heat recovered from the engine jacket and lube oil) producing hot water, and by a high-temperature level (exhaust gases), which feeds the double-effect absorption chiller. The nominal hot water production is equal to 1560 kW, while the nominal exhaust gases production is equal to 2430 kW.

The model for the ICE has been taken from [28]. Therefore, part-load efficiencies for each energy output are considered according to Fig. 5, where the load factor is defined as $L_{ICE} = E_{ICE}/P_{ICE}$. Heat losses (through exhaust, jacketing, lube oil cooling, and radiating) increase in partial load operation and decrease at full load operation due to higher electrical efficiency. The power capacity lower bound is equal to 50% of the nominal power capacity.

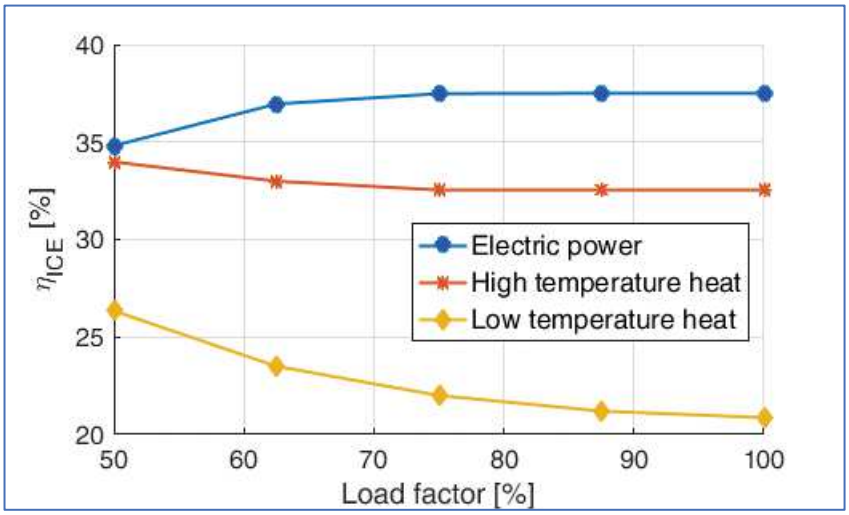

Fig. 5. Part-load efficiencies of the ICE

3.2.2 Absorption chiller

In order to exploit the high-temperature exhaust gases produced by the ICE, a double effect absorption chiller has been taken into account. The unit considered is a Thermax ED 60D [29], which works with a water-lithium bromide solution. The nominal cooling capacity is about 3300 kW and the COP in nominal condition is equal to 1.39.

As suggested by several technical standards (see for instance [30]), the so called locally constant exergetic efficiency (or Carnot efficiency) is used to evaluate chillers performance. By considering also a part-load correction factor, it is possible to take into consideration the effect of both temperature of the heat sources and part-load operations on the chiller COP. In fact, the actual COP of the absorption chiller can be expressed as the product of the ideal COP of the absorption chiller, the exergetic efficiency and a correction factor:

$$COP_{AC} = COP_{AC,id} \cdot \eta_{AC,ex} \cdot CR_{AC} \tag{1}$$

The ideal COP of the absorption chiller is evaluated by means of the average temperature of the chilled water circuit, the cooling water circuit and the exhaust gas circuit.

$$COP_{AC,id} = \frac{T_C}{T_G}\left(\frac{T_G - T_H}{T_H - T_C}\right) \tag{2}$$

The exergetic efficiency method is based on the idea that the thermodynamic quality of the process stays constant over the whole operating temperature range. Thermodynamic quality of a process can be expressed by the exergetic efficiency as ratio between the real COP of the process

and the ideal COP of the Carnot process. The exergetic efficiency is calculated according to the following equation:

$$\eta_{AC,ex} = \frac{COP_{AC,nom}}{COP_{AC,id,nom}}. \tag{3}$$

However, exergetic efficiency is not completely constant in real processes but varies over the range of operation. For this reason, as suggested in [31], a linear interpolation of exergetic efficiencies is applied.

For the machine under consideration, the exergetic efficiency is considered to vary linearly with the temperature at the condenser from 18% (at $t_H = 26.6\,°C$) to 23% (at $t_H = 32\,°C$). These values have been calculated on the basis of the technical specification sheets of the chiller, which provide the COP values at such operating points.

Anyway, the locally constant exergetic method does not consider the exergetic efficiency deterioration at partial load. In order to consider such effect, a correction factor CR, as a function of the load factor, is taken into account, as in [32]. Its trend is shown in Fig. 6. The minimum load factor is: $L_{AC,min} = 20\%$.

3.2.3 Electric chiller

The plant includes also an electric chiller which can cover the peak demand and provides management flexibility, covering the cooling demand when it is not convenient to operate the ICE. The considered unit is a MHI AART 180 [33]. Its nominal cooling capacity is about 6300 kW and its nominal COP is equal to 5.91.

In order to model the electric chiller, the same approach followed for the absorption chiller has been adopted. Therefore, the coefficient of performance is expressed as

$$COP_{EC} = COP_{EC,id} \cdot \eta_{EC,ex} \cdot CR_{EC} \tag{4}$$

where the ideal COP is defined as

$$COP_{EC,id} = \frac{T_C}{T_H - T_C}. \tag{5}$$

In this case, the exergetic efficiency varies linearly with the temperature at the condenser from 27% (at $t_H = 14.5\,°C$) to 52% (at $t_H = 34.5\,°C$) and the correction factor is evaluated on the basis of the technical specification sheets, as shown in Fig. 6. The minimum load factor is: $L_{EC,min} = 10\%$.

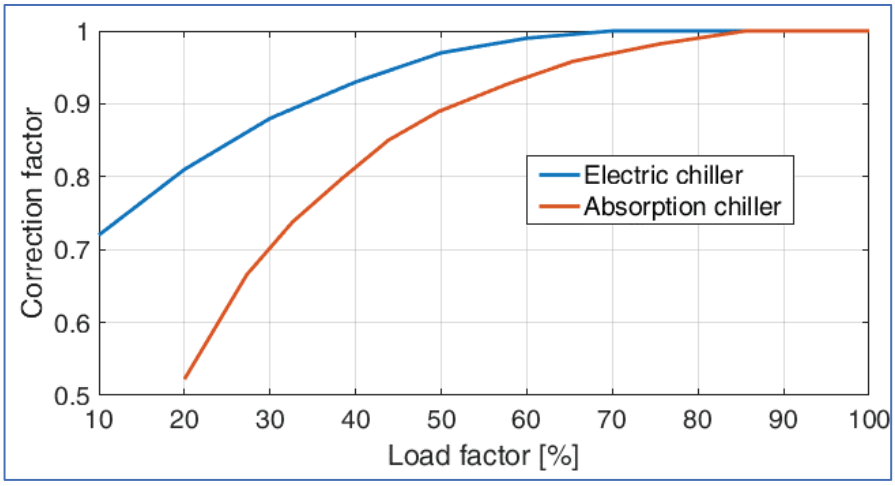

Fig. 6. Chillers correction factors

3.2.4 Boiler

A natural gas boiler for producing hot water has been considered. It has a capacity of 1000 kW, a nominal efficiency of 90% and it has been modelled considering part-load efficiency, as follows [34]:

$$\eta_{boi} = 0.9 \cdot (0.0951 + 1.525 \cdot L_{boi} - 0.6249 \cdot L_{boi}^2). \quad (6)$$

3.2.5 Cooling tower

The cooling tower must dissipate the heat from the condenser/absorber of the absorption chiller, from the condenser of the compression chiller and from the low-temperature circuit of the ICE. The inlet temperature of condenser water (outlet temperature of cooling tower) changes as outdoor weather conditions vary (mainly ambient wet bulb temperature) [35]. To minimize chiller energy use, the condenser water supply temperature set-point should be as low as possible. However, the control set-point should be above the lowest temperature attainable by cooling tower at a certain wet-bulb temperature to avoid the waste of fan energy [36]. To this aim, several cooling tower optimal control strategies have been developed. The so called "fixed approach control method" is a simple and easy strategy to implement for practical applications [37]. Such a method consists in varying the cooling tower air flow rate to maintain a constant temperature difference between the cooling tower outlet water temperature and the ambient air wet bulb temperature. This temperature difference is commonly known as "approach".

As a consequence, the inlet temperature of the cooling water circuit of the chillers can be evaluated as the sum of the ambient air wet bulb temperature and the approach temperature, set at 6 K.

Finally, the electric power consumption due to cooling tower fans is evaluated as 0.005 kW per kW of heat rejection capacity [38].

3.2.6 Ambient conditions

Ambient conditions are considered due to their significant influence on chillers performance. In fact, as seen above, the air wet bulb temperature influences directly the inlet temperature of the cooling water circuit of the chillers, which in turn affects chillers performance.

Known the outdoor dry bulb temperature and relative humidity, the air wet bulb temperature can be easily calculated [39]. Fig. 7 shows dry and wet bulb temperatures by number of occurrence hours of a temperature in the accounted period (from May 1, 2013 to October 13, 2013).

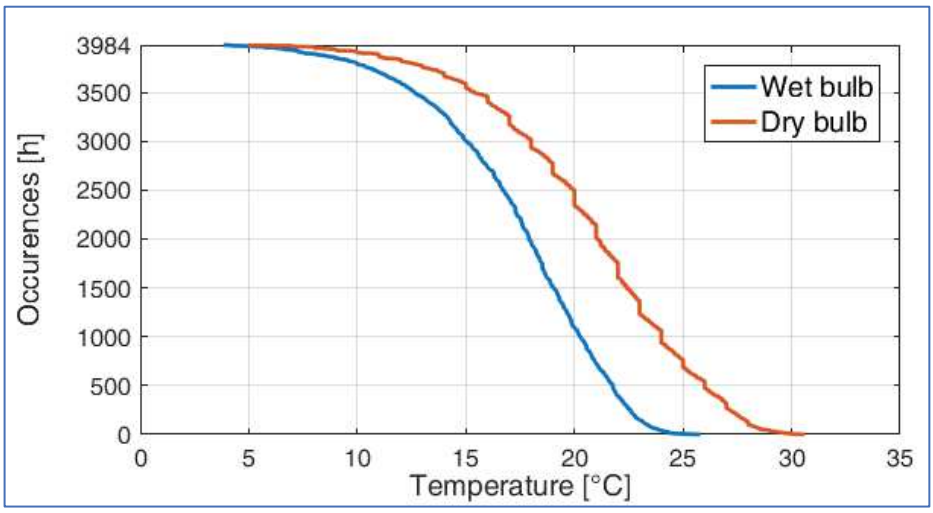

Fig. 7. Occurrence hours of dry and wet bulb temperatures

3.2.7 Energy prices

Both the boiler and the cogeneration unit are fed by natural gas; the fuel cost per unit of thermal energy, on the lower heating value basis, is fixed for the whole period [27]:

$$c_F = 0.04\ €/kWh. \tag{7}$$

The electric grid allows both the sale and the purchase of electric energy. The prices for purchasing and selling electricity vary every hour and the trend of the typical day is shown in Fig. 8. The same profile has been adopted for all the investigated period.

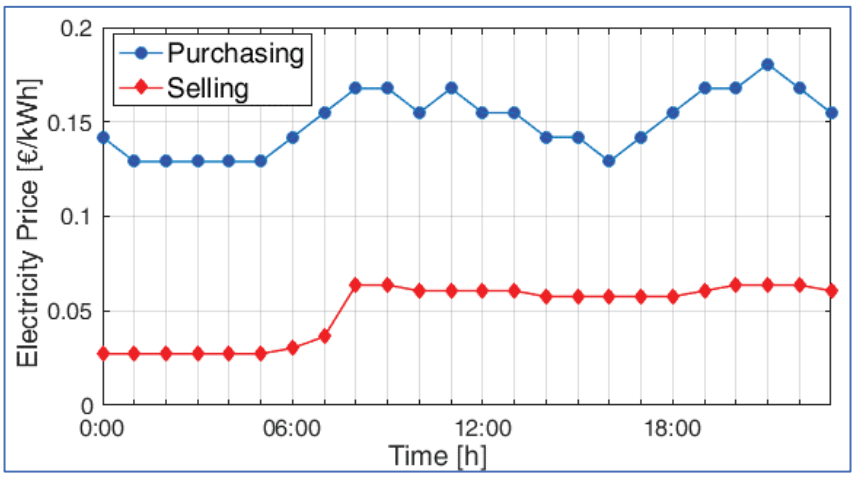

Fig. 8. Electricity prices variation of the typical day (based on [27])

3.2.8 Further considerations on the energy system layout and simulation

The timestep length considered for the plant modelling is 15 minutes and also the continuous operation time constraint for every device is set to 15 minutes. Thus, transient performances of the machines on shorter time scales are neglected and too many on-off cycles are avoided. Indeed, the overall thermal inertia of the distribution network and the start-up time of the machines would not allow a faster control of the energy system. Obviously, since the loads are available on a minute-by-minute basis, they are applied to each simulated timestep as averages of the following 15 minutes.

No thermal energy storages (TESs) have been considered for the system simulation. In fact, even if it is well known that TESs can improve the efficiency of CCHP plants, by providing operational flexibility and reducing peak demand, there are many existing district heating systems that are not equipped with heat storage systems [40], due to both space and economic reasons.

Moreover, we have chosen not to include a large TES because in that case the system configuration would have been unsuitable for the investigation of a real-time operational optimization strategy and the presence of the storage would have imposed a long-term operational strategy. On the other hand, if a small TES (to tackle hourly demand fluctuations) were included, the proposed operational optimization method could still be applied. Indeed, the presence of a small storage would even improve the energy performance of the system under the proposed optimization strategy, by reducing the need for post-strategy operations (described in Section 2.4).

3.3 Other simulated operational strategies

To validate and evaluate the efficiency of the method, the proposed control algorithm is compared to conventional operational strategies and to the ideal optimal management achievable with perfectly accurate forecast of energy demands. These strategies are briefly described in this section.

All the simulations and optimizations are performed using scripts written in MATLAB environment (see Appendix A).

3.3.1 Ideal optimal management

The *Ideal Optimal Management* (IOM) is the operational strategy achievable with a perfect forecast of energy demands. It coincides with the proposed real-time operational strategy, except for the post-strategy design, which is not needed in this ideal case. It represents therefore an ideal benchmark and limit.

3.3.2 Electric energy price based operational strategy

The *Electric Energy Price Based* (EEPB) is an operational strategy that considers only purchasing and selling electricity prices. Since the ratio between the import and export prices of electricity varies considerably during the day (see Fig. 10), a value of switch for the on-off operations of the ICE was set equal to 0.35. Therefore, the cogeneration unit is off from 0:00 to 07:59 and it is on full-load operation from 08:00 to 23:59, every day. This strategy is very similar to the one actually implemented in the real plant [27].

In this case, a post-strategy design is needed too, and it is the same as described in Section 3.4.

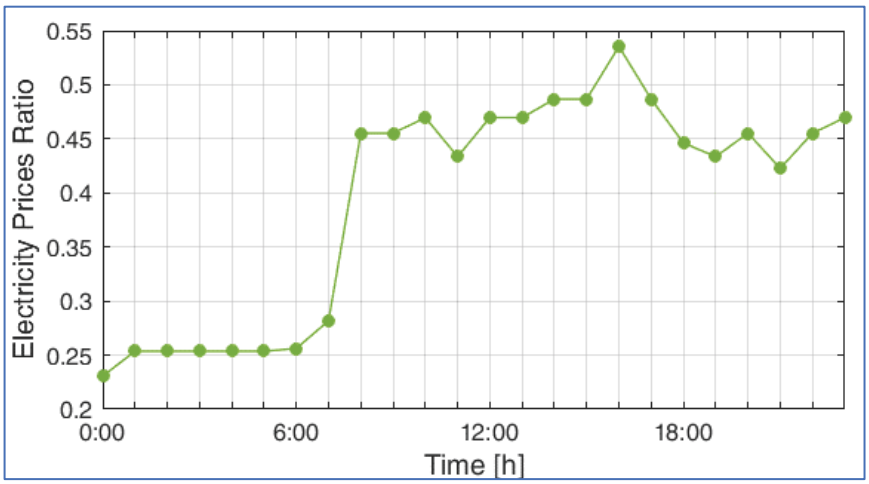

Fig. 10. Electricity prices ratio

3.3.3 Following the thermal load

One of the most typical operating modes of CCHP systems is the *Following the Thermal Load* (FTL) strategy. The FTL mode means that the cogeneration unit is run to have sufficient recovered heat to supply both the cooling and heating requirements. Also in this case, a post-strategy design, as indicated in Section 3.4, may be needed.

3.3.4 ICE continuous full-load operation

The *Continuous Full-Load* (CFL) operation consists of keeping the internal combustion engine always at its maximum load capacity. The usual post-strategy design must be adopted.

3.3.5 Separate production

The *Separate Production* (SP) mode is another reference case, in absence of polygeneration. In the SP mode, the ICE is always off. Therefore, the hot water demand is met by the boiler, while the electric chiller provides the needed chilled water load, purchasing electricity from the external grid. Clearly, the absorption chiller is switched off and no electric energy is sold to the grid.

4. Results and discussion

The results of all the simulated operational strategies for the considered case study are shown in this section. First, the effect of the width of the sliding window on the proposed real-time operational optimization is investigated and then this optimal management is compared to the other operational strategies to verify its performance.

4.1 Effect of different widths of the window for the moving average

In the proposed algorithm, a certain width of the window adopted for the moving average of recent measured energy loads is considered to estimate the forthcoming demand. The choice of the time length affects the performance of the algorithm, since the more accurate is the estimation of the loads in the next timestep, the better the system performance will be.

Several widths have been tested, in order to find the optimal one. Fig. 11 shows the difference between the objective function value (namely, the total energy cost for the whole accounted period, as

defined in paragraph 2.1) obtained under the proposed real-time operational optimization (RTOO) and the ideal cost with perfect forecast of the energy demand (i.e. IOM), for different sliding window widths.

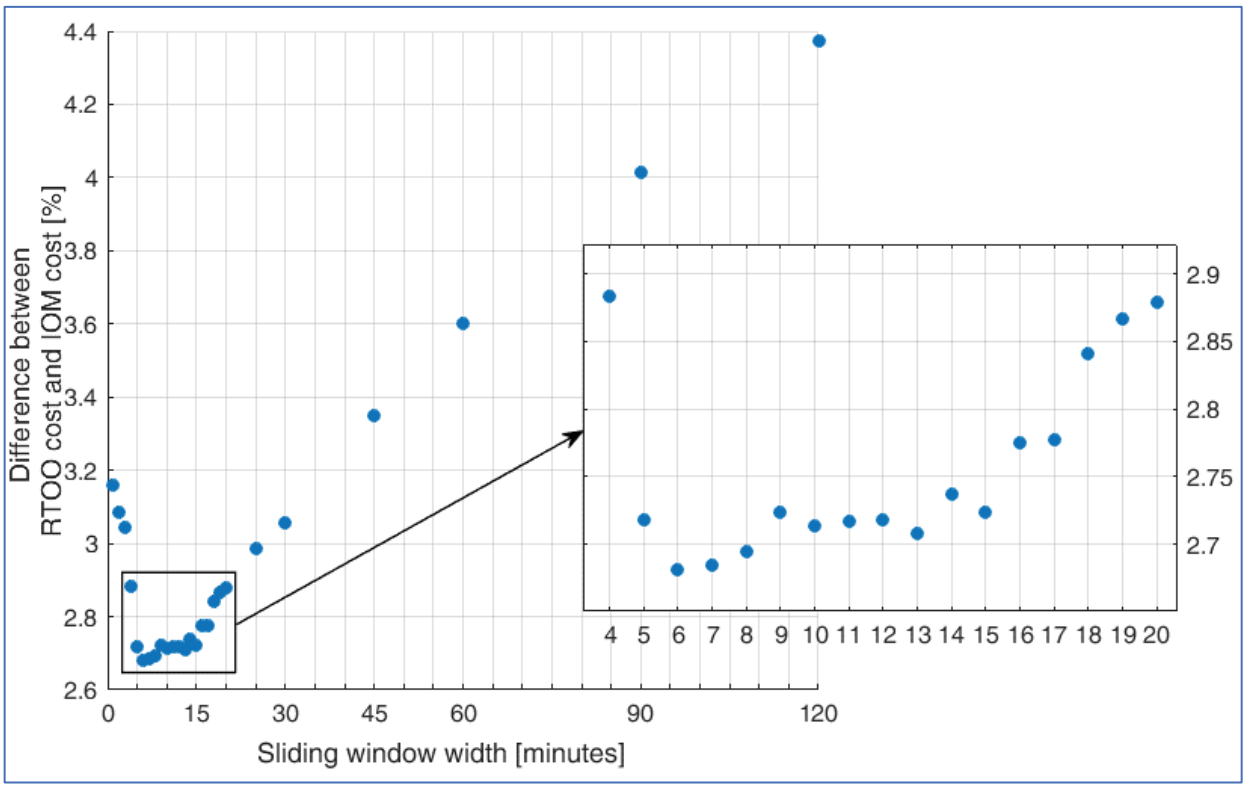

Fig. 11. RTOO cost vs. IOM cost for different sliding window widths

The best performance is achieved for a width of the sliding window of 6 minutes, which provides a 2.68% difference between the proposed optimal management and the ideal one. Nevertheless, this difference varies very slightly in the range from 5 to 15 minutes of width. For this reason, a width of 10 minutes is adopted, as intermediate value. In this way, very recent measurements are filtered, thus preventing outlier fluctuations, and at the same time the moving average effectively estimates the current behavior of the energy demand. From now on, the simulation results concerning the real-time operational optimization refer to a 10-minute width of the sliding window.

4.2 Performance analysis and comparison with other operational strategies

The most significant result, which is shown in Fig. 12, is the comparison of the objective function values obtained under the several simulated operational strategies. First of all, it is clear how the total energy cost obtained under the proposed operational optimization is only slightly above the cost achievable with the ideal forecast of the energy demand. In fact, as already highlighted, the difference between the objective function values of these two operational strategies is below 3%.

The effectiveness of the proposed algorithm is also proven by comparing it with conventional operational strategies. The EEPB management leads to a 13% rise in the energy cost. The FTL and the CFL operations, compared to the RTOO, provide a 22% and 55% increase in the objective function value, respectively. Finally, the separate production mode entails a 58% rise in the energy cost, for the accounted period.

The simulations have clearly shown how the operational strategy considerably influences CCHP system performance. Conventional operational strategies are clearly suboptimal and may even entail performances similar to the ones achievable with a traditional system (i.e. separate production).

It should be noted that the simulations inspect only the summer period, since no detailed energy demand data are available for the rest of the year. Nevertheless, the proposed strategy would be applied in the same way in the winter period and therefore the validity of the methodology is not weakened. In fact, when the main demand consists only of electricity and hot water, the optimal control problem is simpler, since the main concerns are related to the chillers efficiencies.

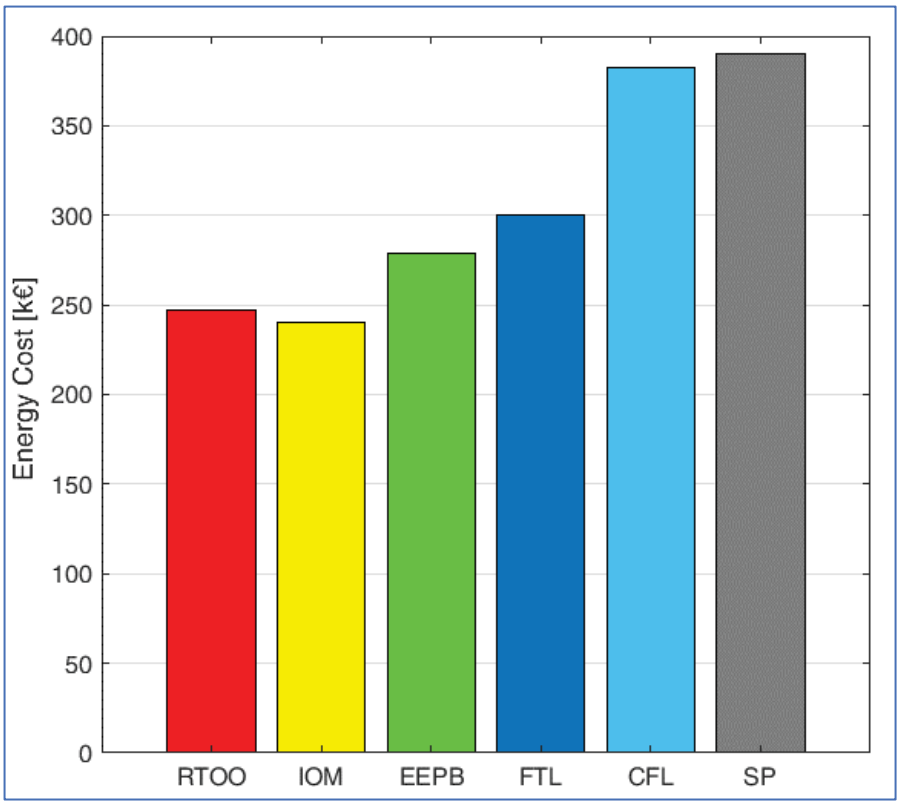

Fig. 12. Operating energy cost of different operational strategies

Figs. 13-16 present some examples of how the energy system works under the simulated operational strategies and what kind of detailed output are available from the simulations. In particular, it is shown how the cooling demand is met, in a typical week.

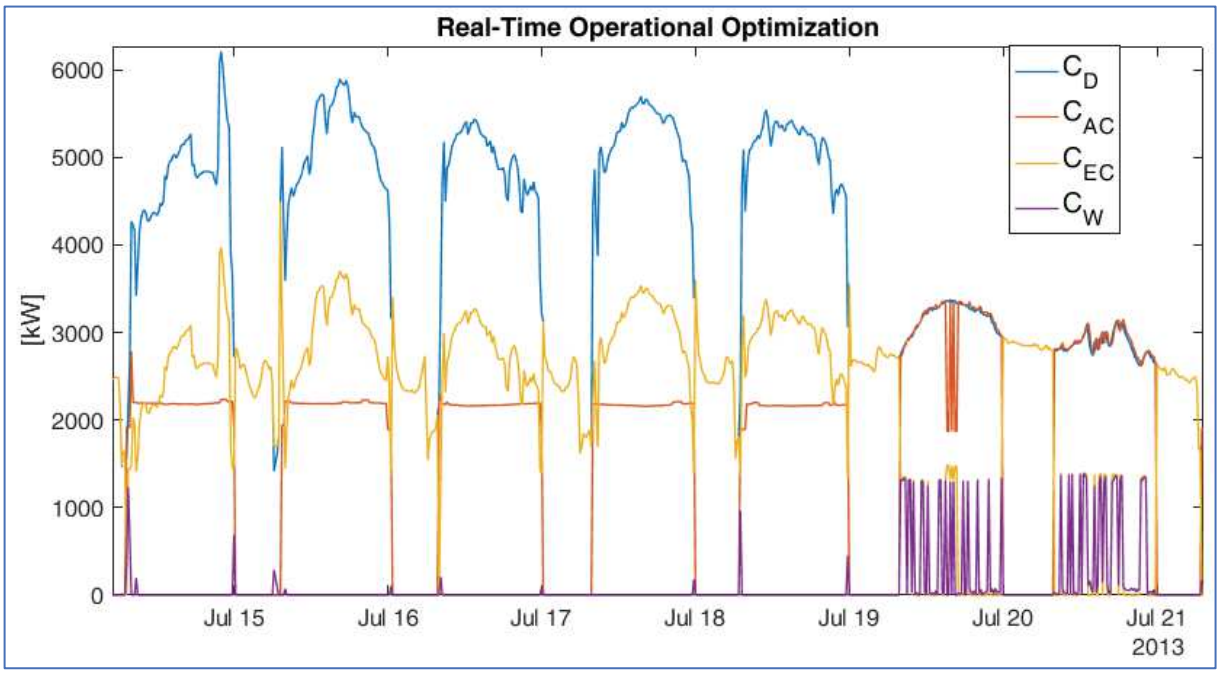

Fig. 13. Simulations results of a typical week (cooling load) under RTOO strategy

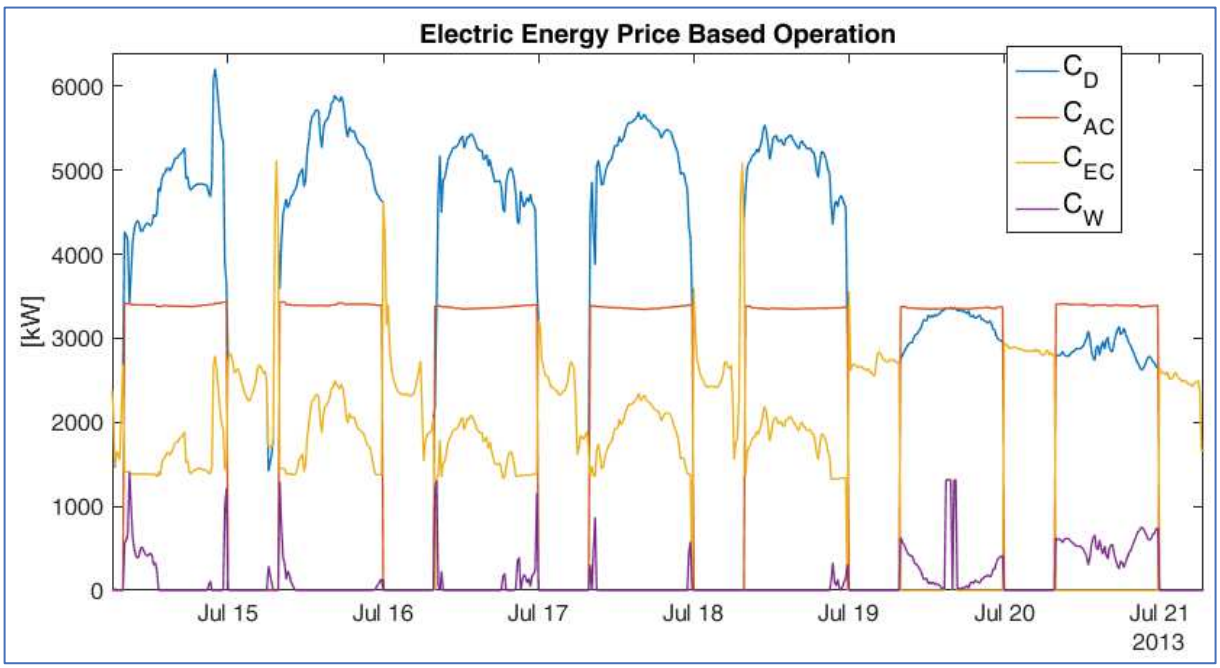

Fig. 14. Simulations results of a typical week (cooling load) under EEPB strategy

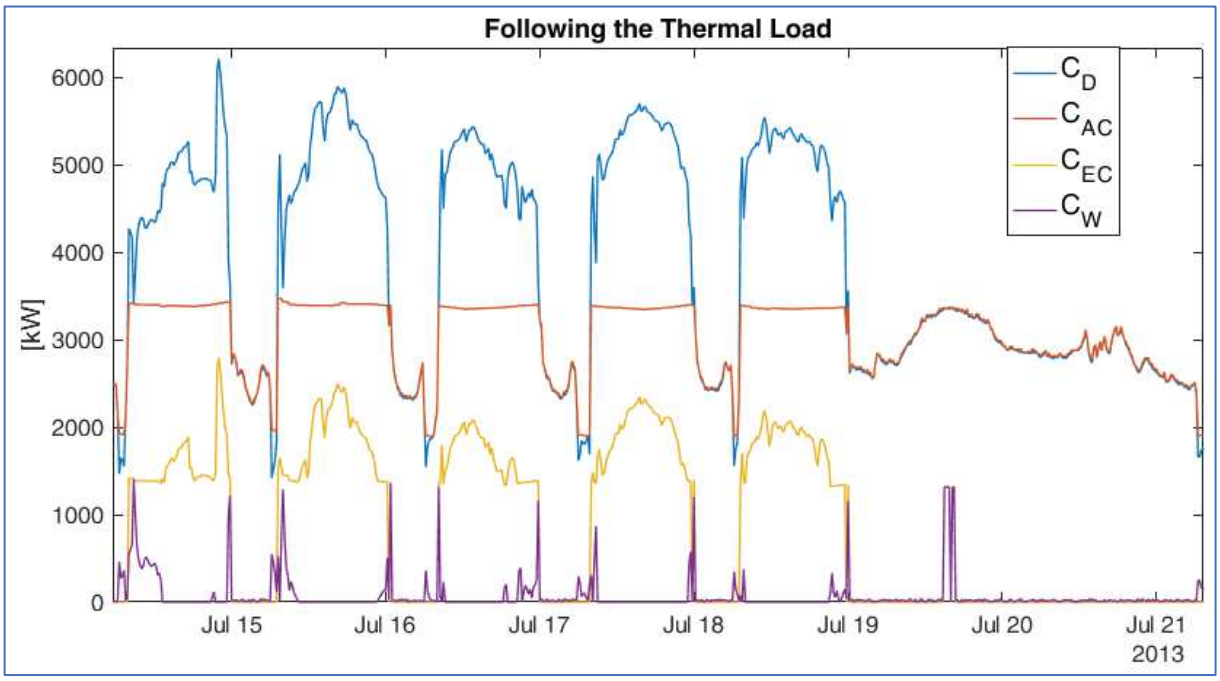

Fig. 15. Simulations results of a typical week (cooling load) under FTL strategy

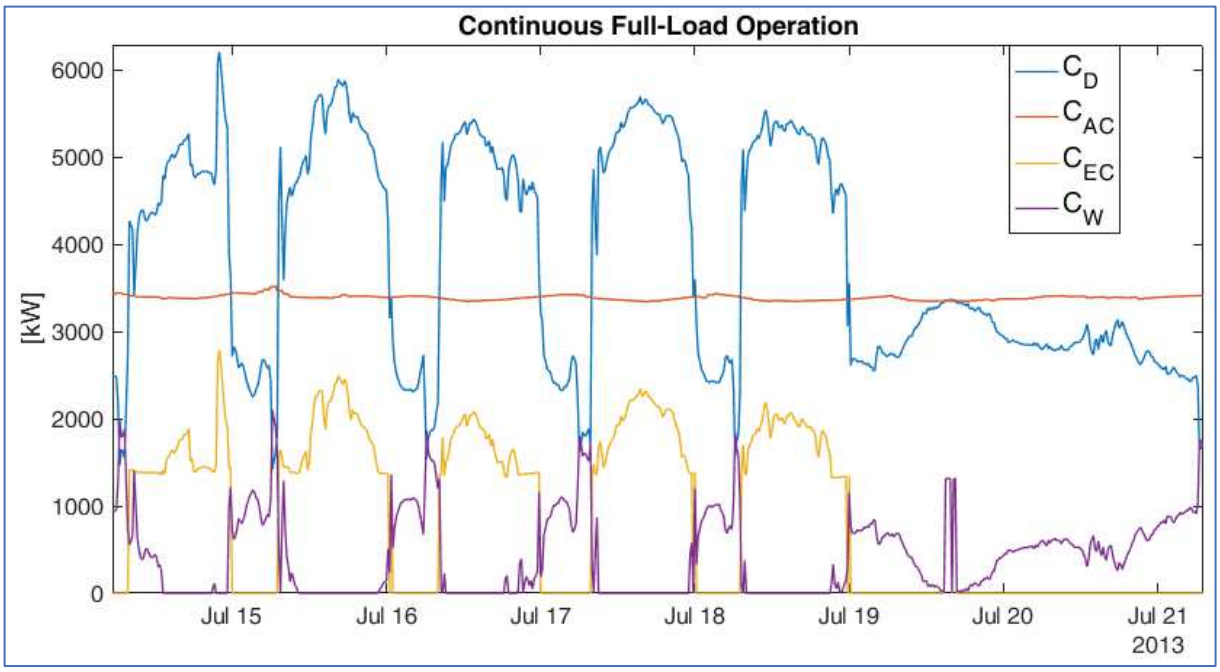

Fig. 16. Simulations results of a typical week (cooling load) under CFL strategy

An interesting indicator to compare different operational strategies is the absorption cooling to cooling load ratio. It represents the ratio between the part of cooling demand met by the absorption chiller and the whole cooling demand, in each 15-minute timestep. Fig. 17 shows how

this indicator varies in the accounted period, for the considered operational strategies. These figures highlight that the optimal absorption cooling to cooling load ratio value stays around 0.5 for a significant number of timesteps, while, under other strategies, most of the ratio values range from 0.6 to 1. This means that, in the present case, the optimal management of the plant requires an even distribution of the cooling load between the absorption and the electric chillers.

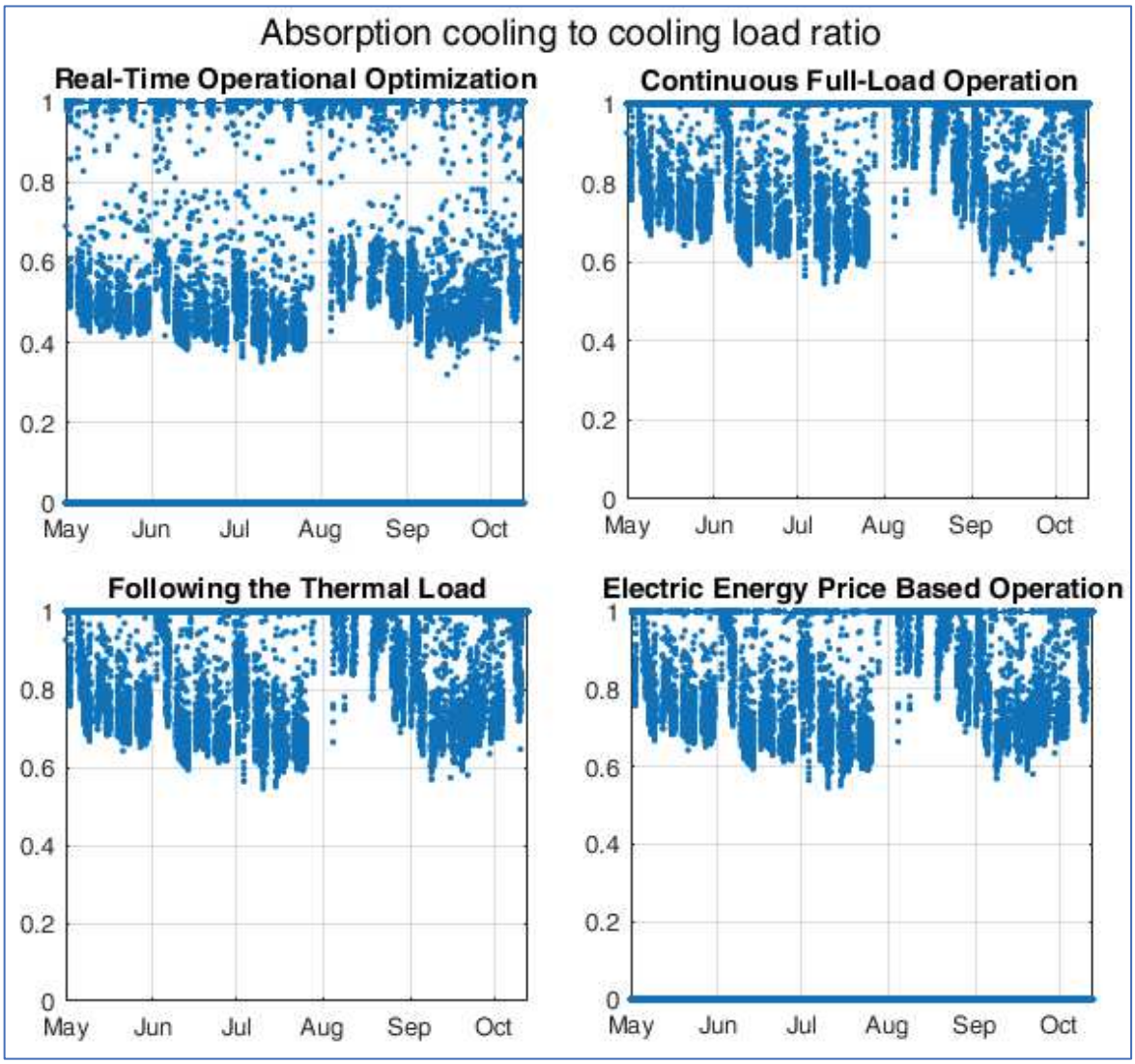

Fig. 17. Variation of the absorption cooling to cooling load ratio under several operational strategies

Moreover, Fig. 18 and 19 show the amount of natural gas consumed, electricity sold to the grid and electricity bought from the grid and related costs, respectively, for all the simulated operational strategies. Apart from the separate production mode, which entails a significant amount

of imported electricity, it can be seen that, compared to conventional operations, the proposed optimal solution reduces both the consumption of natural gas and the supply of electric energy to the grid.

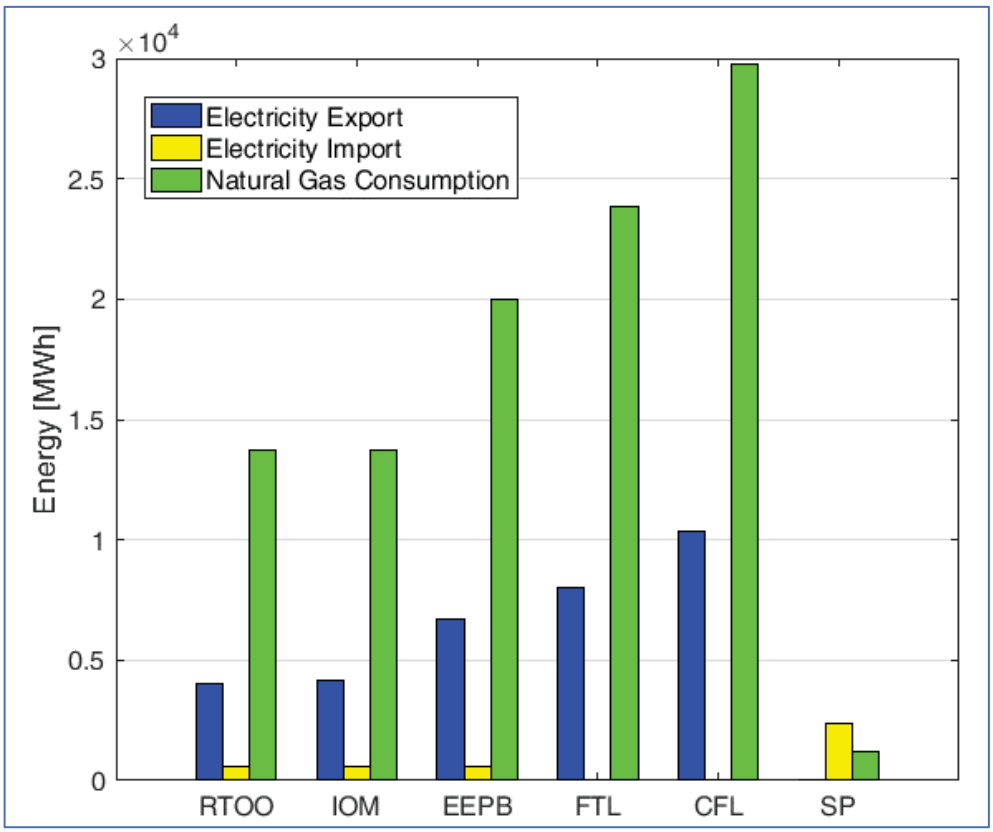

Fig. 18. Energy carriers import/export of different operational strategies

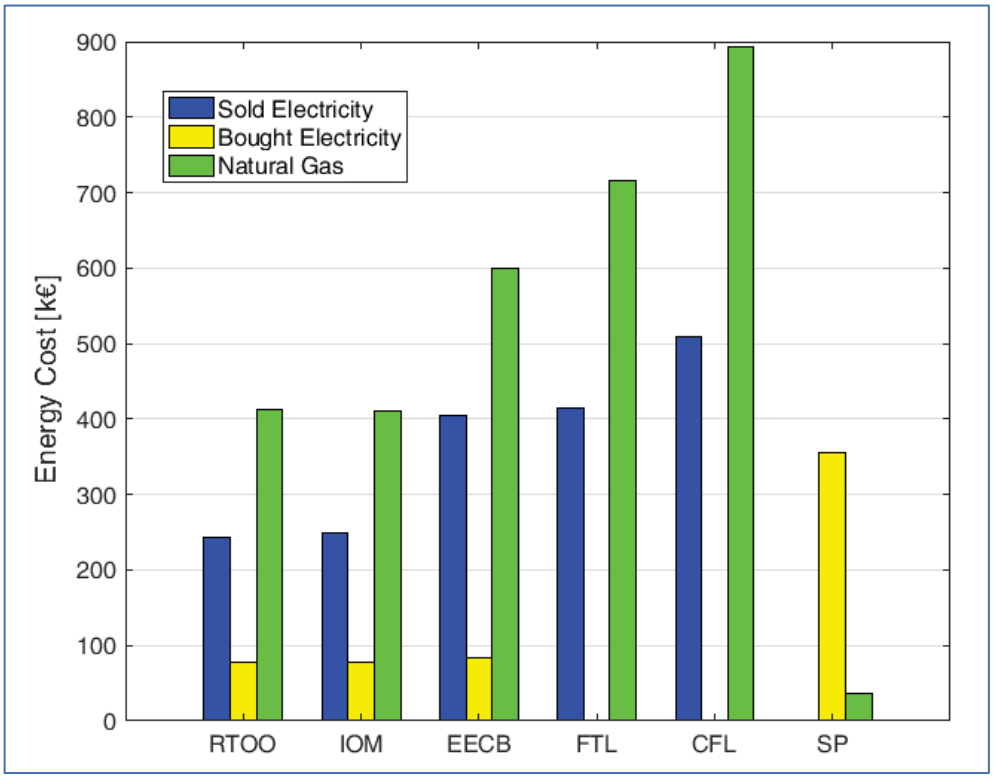

Fig. 19. Energy costs for different operational strategies

Finally, Fig. 20 examines the differences – indeed very limited – between the ideal optimal management and the proposed real-time operational optimization. The average missed saving (i.e. the average cost difference between RTOO and IOM) is shown for each hour of the day. In the same chart, the hourly average chilled water demand is also shown. It can be observed how the more significant missed savings occur when the chilled water demand is higher (and consequently the cost is higher) and when there is a rapid change in chilled water demand. In particular, between 8:00 and 9:00, when the chilled water demand significantly increases in a short time, more than 5 € per hour are wasted, on average. This is due to the fact that discrepancies between the estimated and the actual loads are larger when a rapid change in energy demand happens. On the other hand, no savings are missed during the night, since the ICE is always off and no difference exists between the two operational strategies.

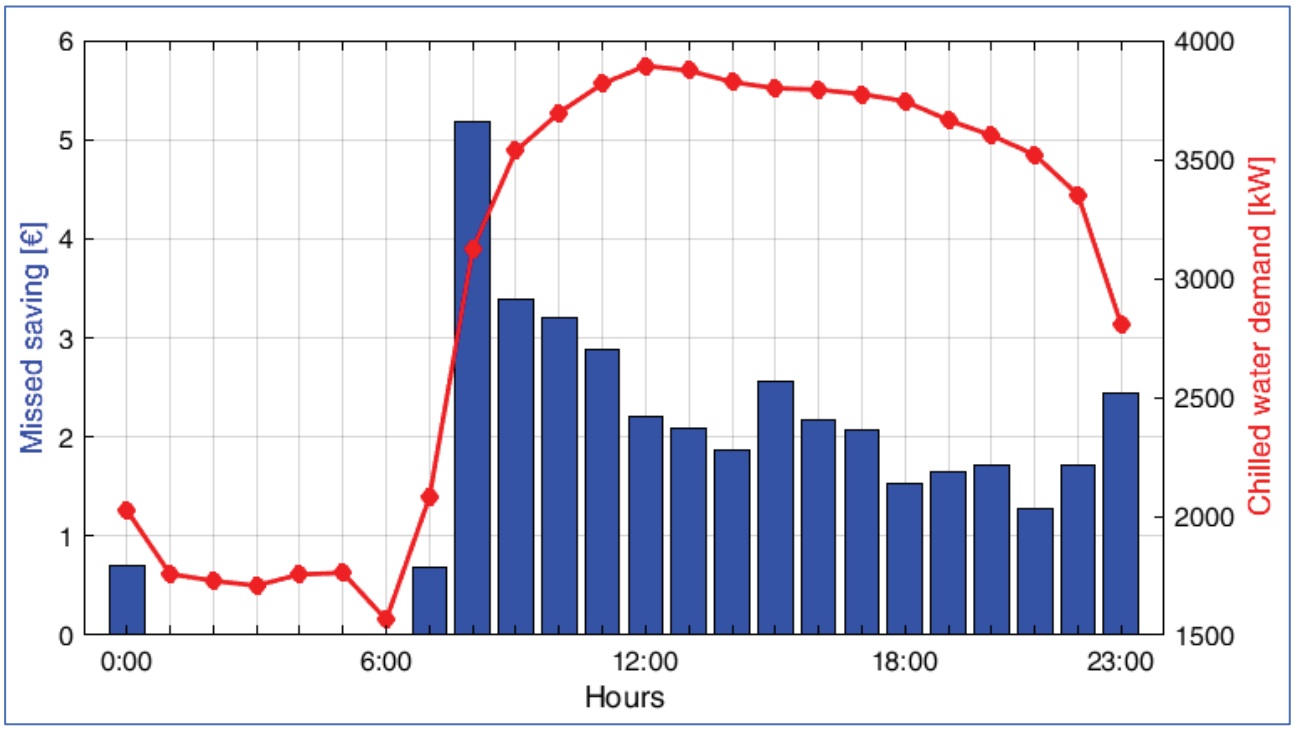

Fig. 20. RTOO missed saving compared to IOM

5. Conclusions

A new real-time operational optimization method for CCHP systems has been proposed in this paper. The method uses real-time measurements of energy demands and ambient conditions to provide the operational signals to the CCHP system that result in minimum energy cost. A moving average analysis has been used to process energy load data and estimate forthcoming demands, so removing the need for weather forecast and energy demand modelling.

The application of the method has been demonstrated with energy demand data from a DHC network close to Barcelona. A detailed modelling of the energy system has been provided, considering partial load behavior of the components and ambient conditions effects. The outlet temperature of cooling tower water changes as outdoor weather conditions vary; consequently, ambient conditions influence chillers performance.

The effectiveness of the method has been clearly proven, since the total operation energy cost achieved with the proposed algorithm is less than 3% higher than the energy cost obtainable with an ideal perfect forecast of the energy demand. Moreover, the proposed methodology has been compared to conventional operational strategies, which imply an increase of the operational costs from 13% to 58%. The optimal width of the sliding window adopted for the moving average has also been identified, and its value is around 10 minutes.

The results suggest that the proposed methodology allows to concretely implement an optimal real-time control strategy in actual applications. It could be successfully and effectively used in real CCHP systems, as long as a monitoring system for measuring real-time energy demands is available.

Future research may focus on: definition of a multi-objective problem (based on environmental, energetic, exergetic indicators), use of real-time data and optimization in case of integration with renewable energy sources and thermal storages.

Appendix A. Supplementary material

The MATLAB code associated with this article is available as supplementary material.

Nomenclature

Acronyms

CFL	Continuous full-load
EEPB	Electric energy price based
FTL	Following the thermal load
IOM	Ideal optimal management
RTOO	Real-time operational optimization
SP	Separate production

Parameters

c	Unit cost, €/kWh
COP	Coefficient of performance, dimensionless
CR	Part-load correction factor, dimensionless
EC	Energy cost, €
f	Electric energy consumption per unit of rejected heat, dimensionless
η	Efficiency, dimensionless

Continuous variables

C	Cooling energy, kWh
E	Electric energy, kWh

F	Energy content of the consumed fuel, kWh
L	Load factor, dimensionless
Q	Thermal energy, kWh
T	Absolute temperature, K
t	Temperature, °C
W	Waste heat, kWh

Binary variables

δ	On-off state

Subscripts

AC	Absorption chiller
boi	Boiler
ICE	Internal combustion engine
id	Ideal
C	Cold
CT	Cooling tower
D	Demand
E	Electric
EC	Electric chiller
ex	Exergetic
F	Fuel
G	Generator
H	Hot
HT	High-temperature level

LT	Low-temperature level
min	Minimum
nom	Nominal (L=1)
P	Purchased
PEG	Electricity purchased by the grid
Q	Thermal
S	Sold
SEG	Electricity sold to the grid
W	Wasted

References

[1] Pérez-Mora N, Lazzeroni P, Martinez-Moll V, Repetto M. Optimal Management of a complex DHC plant. Energy Convers Manage 2017;145:386-97.

[2] Li H, Svendsen S. District Heating Network Design and Configuration Optimization with Genetic Algorithm. J Sustain Dev Energy Water Environ Syst 2013;1:291-303.

[3] Afzali SF, Mahalec V. Optimal design, operation and analytical criteria for determining optimal modes of CCHP with fired HRSG, boiler, electric chiller and absorption chiller. Energy 2017;139:1052-65.

[4] Liu M, Shi Y, Fang F. A new operation strategy for CCHP systems with hybrid chillers. App Energy 2012;95:164-73.

[5] Song X, Liu L, Zhu T, Wu Z. Comparative analysis on operation strategies of CCHP system with cool thermal storage for a data center. App Therm Eng 2016;108:680-88.

[6] Murugan S, Horák B. Tri and polygeneration systems – A review. Ren Sust Energy Rev 2016;60:1032–51.

[7] Arcuri P, Florio G, Fragiacomo P. A Mixed integer programming model for optimal design of trigeneration in a hospital complex. Energy 2007;32-1430-47.

[8] Guo L, Liu W, Cai J, Hong B, Wang C. A two-stage optimal planning and design method for combined cooling, heat and power microgrid system. Energy Convers Manage 2013;74:433-45

[9] Elsido C, Bischi A, Silva P, Martelli E. Two-stage MINLP algorithm for the optimal synthesis and design of networks of CHP units. Energy 2017;121:403-26.

[10] Arcuri P, Beraldi P, Florio G, Fragiacomo P. Optimal design of a small size trigeneration plant in civil users: a MINLP (Mixed Integer Non Linear Programming Model), Energy 2015;80:628-41.

[11] Franco A, Versace M. Multi-objective optimization for the maximization of the operating share of cogeneration system in District Heating Network. Energy Convers Manage 2017:139:33-44.

[12] Li L, Mu H, Li N, Li M. Analysis of the integrated performance and redundant energy of CCHP systems under different operation strategies. Energy Build 2015;99:231-42.

[13] Ortiga J, Bruno JC, Coronas A. Operational optimization of a complex trigeneration system connected to a district heating and cooling network. Appl Therm Eng 2013;50:1536-42.

[14] Bischi A, Taccari L, Martelli E, Amaldi E, Manzolini G, Silva P, Campanari S, Macchi E. A detailed MILP optimization model for combined cooling heat and power system operation planning. Energy 2014;74:12-26.

[15] Ünal AN, Ersöz I, Kayakutlu G. Operational optimization in simple tri-generation systems. Appl Therm Eng 2016;107:175-83.

[16] Liu M, Shi Y, Fang F. Optimal power flow and PGU capacity of CCHP systems using a matrix modeling approach. Appl Energy 2013;102:794-802.

[17] Fang T, Lahdelma R, Optimization of combined heat and power production with heat storage based on sliding time window method. Appl Energy 2016;162:723-32.

[18] Luo Z, Wu Z, Li Z, Cai H, Li B, Gu W, A two-stage optimization and control for CCHP microgrid energy management. Appl Therm Eng 2017;125:513-22.

[19] Cho H, Luck R, Eksioglu SD, Chamra LM. Cost-optimized real-time operation of CHP systems. Energy Build 2009;41:445-51.

[20] Yun K, Cho H, Luck R, Mago PJ, Real-time combined heat and power operational strategy using a hierarchical optimization algorithm, Proceedings of 2011 IMechE Vol. 225 Part A: J Power and Energy.

[21] Cho H, Smith AD, Mago P. Combined cooling, heating and power: A review of performance improvement and optimization. Appl Energy 2014;136:168-85.

[22] Al Moussawi H, Fardoun F, Louahlia-Gualous H. Review of tri-generation technologies: Design evaluation, optimization, decision-making, and selection approach. Energy Convers Manage 2016;120:157-96.

[23] Urbanucci L, Testi D. Optimal integrated sizing and operation of a CHP system with Monte Carlo risk analysis for long-term uncertainty in energy demands. Energy Convers Manage 2018;157C:307-316.

[24] Shi Y, Liu M, Fang F. Combined Cooling Heating, and Power System. Modelling, Optimization, and Operation. Wiley; 2017.

[25] Liu M, Shi Y, Fang F. Load forecasting and operation strategy design for CCHP systems using forecasted loads, IEEE Transactions on control system technology, 2015; 1672:1684-23

[26] Conte B, Bruno JC, Coronas A. Optimal cooling load sharing strategies for different types of absorption chillers in trigeneration plants. Energies, 2016;9(8):573-88.

[27] Conte B. A MILP model for the optimal cooling load sharing in a trigeneration power plant, Master Thesis in Energy Engineering. University of Pisa; 2015. <https://etd.adm.unipi.it/theses/available/etd-02092016-110745/unrestricted/Tesi_Finale.pdf> [accessed 17.10.17].

[28] Ebrahimi M, Keshavarz A. Combined Cooling, Heating and Power: Decision-Making, Design and Optimization. Elsevier; 2015.

[29] <http://www.thermaxglobal.com/pdf/Exhaust-Driven.pdf> [accessed 17.10.17].

[30] EN 15316-4-2, Heating systems in buildings - Method for calculation of system energy requirements and system efficiencies - Part 4-2: Space heating generation systems, heat pump systems. Brussels: European Committee for Standardization (CEN); 2008.

[31] Genkinger A. Jahresbericht EFKOS – Effizienz kombinierter Systeme mit Wärmepumpe, im Auftrag des BFE, Fachhochschule Nordwestschweiz FHNW, Muttenz, 2012, Schweiz

[32] UNI/TS 11300-4:2012, Energy performance of buildings – Part 4: Renewable energy and other generation systems for space heating and domestic hot water production. Milan: Italian National Unification; 1994.

[33] <http://www.mhi-mth.co.jp/catalogue.html> [accessed 17.10.17].

[34] Zhou Z, Liu P, Li Z, Pistikopoulos EN, Georgiadis MC. Impacts of equipment off-design characteristics on the optimal design and operation of combined cooling, heating and power systems. Comput Chemical Eng 2013;48:40-47.

[35] Liu Z, Tan H, Luo D, Yu G, Li J, Li Z. Optimal chiller sequencing control in an office building considering the variation of chiller maximum cooling capacity. Energy Build 2017;140:430-442.

[36] Wang S. Intelligent buildings and building automation. Spon Press; 2010.

[37] Ma Z, Wang S, Xu X, Xiao F. A supervisory control strategy for building cooling water systems for practical and real time applications. Energy Convers Manage 2008;49:2324-2336.

[38] DiPippo R. Geothermal Power Generation: Developments and Innovation. Woodhead Publishing; 2016.

[39] Stull R. Wet-Bulb Temperature from Relative Humidity and Air Temperature. American Meteorological Society; 2011.

[40] Noussan M. Performance indicators of District Heating Systems in Italy – Insights from a data analysis. Appl Therm Eng 2018;134:194-202.